Chapter 4

Lateral earth pressure

4.1 Introduction

Problems of deep excavation, no matter if stability analysis (Chapter 5), stress analysis or deformation analysis (Chapters 6–8), entail the distribution of earth pressures. Though introductory books on soil mechanics or foundation engineering have discussed quite a few earth pressure theories along with many examples, a systematic organization is lacking. Some important points may not be sufficiently emphasized. In actual analyses, a wrong choice of earth pressure theory may lead to an uneconomical or even unsafe design. This chapter is going to do systematic organization and to simplify the complicated calculations for excavation analyses and design. Most of the methods introduced here have been frequently used in engineering practice though they have not been introduced in general textbooks. Common examples of the calculation of earth pressures, since many exist in books on soil mechanics and foundation engineering, are not to be discussed in the chapter but will be left in the exercise problems at the end of the chapter. The exercise problems are mostly those that have been encountered in engineering practice.

4.2 Lateral earth pressure at rest

Figure 4.1 shows a vertical retaining wall whose height is H. Suppose friction does not exist between the retaining wall and the soil. When the wall is not allowed to move, the stresses at depth, z, below the ground surface are under elastic equilibrium with no shear stress. Supposing the vertical effective overburden stress is σ'_v, and lateral effective stress σ'_h, then:

$$\sigma'_h = K_0 \sigma'_v \tag{4.1}$$

where K_0 = coefficient of lateral earth pressure at rest.

The total lateral stress is

$$\sigma_h = \sigma'_h + u \tag{4.2}$$

where u is porewater pressure, the sum of the static water pressure and excess porewater pressure.

For cohesionless soils, K_0 can be estimated by Jaky's (1944) equation:

$$K_0 = 1 - \sin \phi' \tag{4.3}$$

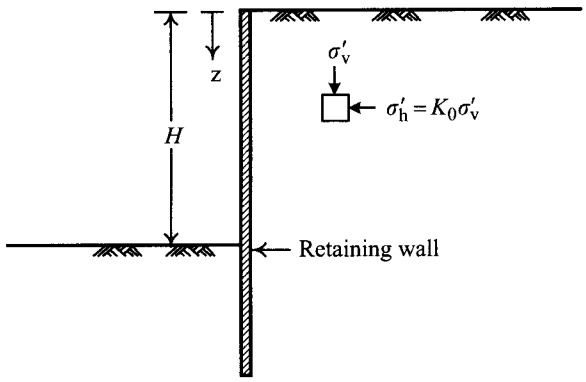

Figure 4.1 Lateral earth pressure at rest.

where ϕ' = effective internal angle of friction (also called the effective angle of shearing resistance or the drained angle of shearing resistance).

When cohesionless soils are in the unloading or preconsolidated states (i.e. overconsolidated), K_0 can be expressed by the following equation (Alpan 1967; Schmidt 1967):

$$K_{0,OC} = K_{0,NC}(OCR)^{\alpha} \tag{4.4}$$

where $K_{0,OC}$ = coefficient of lateral earth pressure at rest of overconsolidated soils with overconsolidation ratio, OCR; $K_{0,NC}$ = coefficient of lateral earth pressure at rest of a normally consolidated soil; α = empirical coefficient, $\alpha \approx \sin\phi'$.

Ladd *et al.* (1977) suggested that K_0 of normally consolidated cohesive soils can also be estimated by Eq. 4.3. For overconsolidated soils, Ladd *et al.* (1977) suggested that K_0 can be obtained by Eq. 4.4, where the α-value decreases slightly with the increase of the plasticity index (PI). For example, when PI = 20, α = 0.4; when PI = 80, α = 0.32. The α-value does not actually vary much. When applied to practical cases, we can select an appropriate α-value according to the above experimental results.

Generally speaking, for normally consolidated cohesive or cohesionless soils, Eq. 4.3 can produce quite satisfactory results. For overconsolidated soils, nevertheless, cohesive and cohesionless alike, the results from Eq. 4.4 are relatively inaccurate. One of the reasons is that the formation process of overconsolidated soils is complicated. To obtain the most appropriate K_0-value, the best way is to carry out an in situ test.

4.3 Rankine's earth pressure theory

Rankine (1857) developed a theory of lateral earth pressure in conditions of failure in front of and in back of a retaining wall on the basis of the concept of plastic equilibrium.

As Figure 4.2a shows, the parameters of soil strength both in front of and in back of the retaining wall are c and ϕ. Suppose there exists no friction between the retaining wall and the soil and the earth pressure both in front of and in back of the retaining wall is at K_0 before

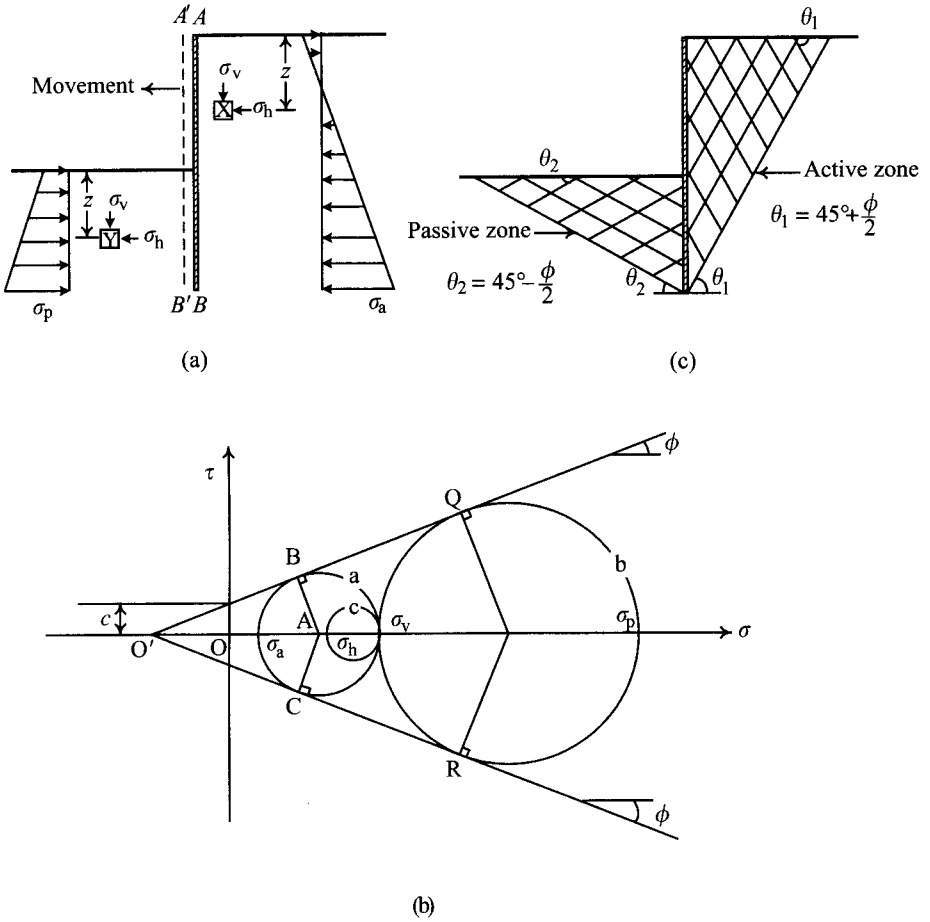

Figure 4.2 Rankine's earth pressure theory.

the retaining wall moves. The vertical stress, σ_v, at X and Y near the wall and at depth, z, below the ground surface are the same and the stress conditions can be represented by the Mohr's circle (circle **c**) in Figure 4.2b. Due to the earth pressure on the back of the retaining wall, the wall is pushed away to A′B′. The horizontal stress decreases while the vertical stress condition is unchanged. The Mohr's circle grows larger and will intersect at a point with the failure envelope when the soil at X is at failure. The type of failure is called active failure and the lateral earth pressure on the retaining wall is called active earth pressure, as is represented by σ_a on circle **a**. Therefore

$$\sin\phi = \frac{AB}{AO'} = \frac{AB}{OO' + OA} = \frac{(\sigma_v - \sigma_a)/2}{c\cot\phi + (\sigma_v + \sigma_a)/2}$$

which can be simplified as follows:

$$\sigma_a = \sigma_v \frac{1-\sin\phi}{1+\sin\phi} - 2c\frac{\cos\phi}{1+\sin\phi} \tag{4.5}$$

$$= \sigma_v \tan^2\left(45° - \frac{\phi}{2}\right) - 2c\tan\left(45° - \frac{\phi}{2}\right)$$

$$= \sigma_v K_a - 2c\sqrt{K_a} \tag{4.5a}$$

where K_a = Rankine's coefficient of lateral active earth pressure = $\tan^2(45° - \phi/2)$.

According to Mohr's failure theory, there forms a failure zone behind the retaining wall, which is called the active failure zone where the soil is all at failure. The failure surfaces all form angles of $(45° + \phi/2)$ with the horizontal (see Figure 4.2c). From Figure 4.2b, the earth pressure distribution behind the retaining wall can be obtained at the theoretical level as shown in Figure 4.2a.

Figure 4.2a shows that the earth pressure behind the wall pushes the wall forward. In front of the wall, at depth z below the ground surface, the lateral stress at Y increases while the vertical stress σ_v stays constant. Thus, the corresponding Mohr's circle grows smaller. When the lateral stress exceeds σ_v, however, the Mohr's circle begins to grow larger. When the Mohr's circle intersects at a point with the failure envelope, the soil at Y will fail. The above type of failure is called passive failure and the lateral earth pressure acting on the front of the wall is called passive earth pressure, which can be represented by σ_p on circle **b**. Following similar derivations used in Eq. 4.5, we can obtain:

$$\sigma_p = \sigma_v \tan^2\left(45° + \frac{\phi}{2}\right) + 2c\tan\left(45° + \frac{\phi}{2}\right) \tag{4.6}$$

$$= \sigma_v K_p + 2c\sqrt{K_p} \tag{4.6a}$$

where K_p is called Rankine's coefficient of lateral passive earth pressure = $\tan^2(45° + \phi/2)$.

Similarly, according to Mohr's failure theory, the failure zone where passive failures happen is called the passive failure zone. The soil in the area is all at failure, whose failure surfaces form angles of $45° - \phi/2$ with the horizontal plane, as shown in Figure 4.2c.

Suppose the wall moves forward by such a great distance that the soil before the wall is completely at passive failure (see Section 4.5.1). The distribution diagram of the passive earth pressures before the wall is also as shown in Figure 4.2a.

According to the principle of effective stress, soil failures are exclusively related to the effective stress, and they have nothing to do with the total stress. Thus, Mohr's circles of failure should be expressed in terms of the effective stress and the failure envelope in Figure 4.2b should be expressed in terms of the effective cohesion (c') and the effective internal angle of friction (ϕ'). Eqs 4.5 and 4.6 should be rewritten in terms of the effective stress as follows:

$$\sigma'_a = \sigma'_v \tan^2\left(45° - \frac{\phi'}{2}\right) - 2c'\tan\left(45° - \frac{\phi'}{2}\right) \tag{4.7}$$

$$= \sigma'_v K_a - 2c'\sqrt{K_a} \tag{4.7a}$$

$$\sigma'_p = \sigma'_v \tan^2\left(45° + \frac{\phi'}{2}\right) + 2c' \tan\left(45° + \frac{\phi'}{2}\right) \tag{4.8}$$

$$= \sigma'_v K_p + 2c'\sqrt{K_p} \tag{4.8a}$$

where the coefficients of the active and the passive earth pressure are separately $K_a = \tan^2(45° - \phi'/2)$ and $K_p = \tan^2(45° + \phi'/2)$.

The angle between the active failure surface and the horizontal plane is $45° + \phi'/2$ and that between the failure passive surface and the horizontal plane is $45° - \phi'/2$.

As Figure 4.3a shows, suppose the soil in front of and in back of the wall is all saturated and both σ_v and the undrained shear strength (s_u) of soil at X and Y are the same (Note: as a matter of fact, the soil at X and Y may not be the same). The soil is at the K_0-condition initially, corresponding to Mohr's circle **a**. Due to the gradual movement toward A′B′, σ_h decreases little by little (σ'_h decreases as well). Shear begins to act on X (under undrained conditions) and excess porewater pressure is produced. When the corresponding Mohr's circle of σ'_h and σ'_v (circle **b**) intersects at a point with the failure envelope, the soil will fail. If we suppose the

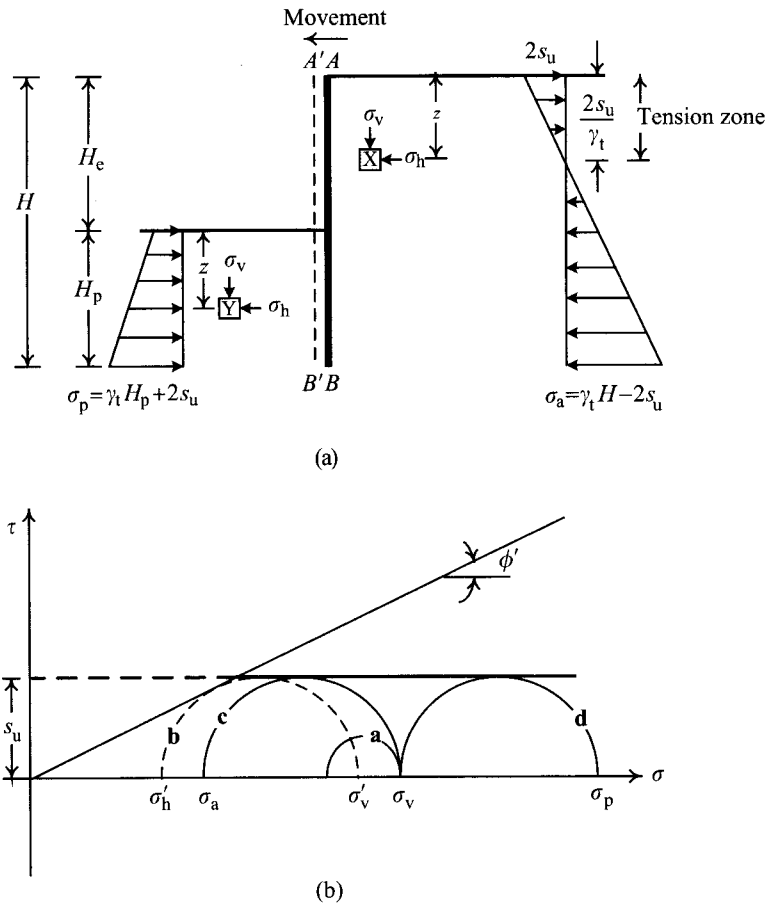

Figure 4.3 Active and passive earth pressures under undrained conditions.

corresponding Mohr's circle of total stress at failure is circle **c**, according to the geometric relationships as shown in Figure 4.3b, the active earth pressure on the wall is:

$$\sigma_a = \sigma_v - 2s_u \tag{4.9}$$

where s_u is the undrained shear strength.

According to Eq. 4.9, we can obtain the theoretical distribution of earth pressure as shown in Figure 4.3a. Soil, however, can not actually bear tension. It needs modification for practical applications. For more discussion, please see Section 4.6.

Concerning the soil at Y in front of the wall, the movement of the wall from AB to A′B′ increases the lateral earth pressure σ_h (σ_h' increases as well), and makes the Mohr's circle grow smaller. When σ_h exceeds σ_v, the Mohr's circle begins to grow larger. Shear begins to act on the soil and produces excess porewater pressure with the increase of σ_h. When the Mohr's circle of the effective stress, constituted by the σ_h' and σ_v', intersects at a point with the Mohr failure envelope, the soil will fail. What is noteworthy, the s_u values at X and Y are the same, as shown in Figure 4.3a. Thus, the corresponding Mohr's circles of the effective stress of X and Y at failure should be identical as well, though the major effective principal stress and the minor effective principal stress are reversed. The passive earth pressure can be obtained from the geometric relationships in Figure 4.3b as follows:

$$\sigma_p = \sigma_v + 2s_u \tag{4.10}$$

According to Eq. 4.10, we can obtain the distribution of passive earth pressures in front of the wall, as shown in Figure 4.3a.

Suppose Eqs 4.5 and 4.6 could apply to the total stress. Observing the failure envelope of total stress in Figure 4.3b parallels the x-axis, its slope is zero, that is, $\phi = 0$. It seems workable to substitute $\phi = 0$ into Eqs 4.5 and 4.6 and the results of σ_a and σ_p will turn out to be identical with those from Eqs 4.9 and 4.10. The procedure is certainly erroneous according to the principle of effective stress but the results are correct.

According to the principle of effective stress, soil behaviors relate only to the effective stress and have nothing to do with the total stress. Eqs 4.5 and 4.6 can only apply to effective stress and have no explanatory value for total stress. At the theoretical level, both the active and passive earth pressures of saturated clay should conform to the principle of effective stress and should only be derived according to it. Though Eqs 4.9 and 4.10 are expressed in total stress, they are derived following the principle of effective stress, as shown in Figure 4.3. Concerning the related theory, please refer to Section 2.8.1 in Chapter 2.

The Mohr failure envelope of total stress obtained from the UU test on unsaturated cohesive soils does not parallel the x-axis, that is, $\phi \neq 0$. Theoretically, the active and passive earth pressure on the retaining wall should also be computed following the principle of effective stress. However, for simplification, the lateral earth pressures are usually computed by Eqs 4.5 and 4.6 in engineering practice, considering the theoretical complication of unsaturated cohesive soils, studies of which are to be done yet.

Rankine's earth pressure theory applies, originally, only to problems under specific conditions: vertical and smooth wall backs, homogeneous soil, level grounds, and no surcharge. Real excavation problems, however, are seldom that pure and simple. Some modifications are necessary when applying the theory to practical cases (see Section 4.6).

4.4 Coulomb's earth pressure theory

Coulomb's earth pressure theory (1776) assumes that soil in back of the retaining wall is homogeneous and cohesionless, the failure surface is a plane, the wedge between the wall and the failure surface is rigid material, and the weight of the wedge, the reaction of the soil and the reaction of the wall are in equilibrium.

Figure 4.4a shows a retaining wall of height H, retaining a soil with an angle of friction ϕ and an angle of friction between the wall and soil δ. BC is an assumed failure surface, which intersects with the horizontal plane at an angle of α. Figure 4.4b illustrates the force polygon formed by the reaction of the wall against the wedge (P), the reaction of soil against the wedge (R), and the weight of soil (W). The directions of P and R are determined, assuming that the wall has a tendency to fall forward and the wedge ABC downward. As shown by the force polygon in Figure 4.4b, we can derive the following equation:

$$\frac{W}{\sin(90^\circ + \theta + \delta - \alpha + \phi)} = \frac{P}{\sin(\alpha - \phi)} \tag{4.11}$$

$$P = \frac{W \sin(\alpha - \phi)}{\sin(90^\circ + \theta + \delta - \alpha + \phi)} \tag{4.12}$$

$$= \frac{1}{2}\gamma H^2 \left[\frac{\cos(\theta - \alpha)\cos(\theta - \beta)\sin(\alpha - \phi)}{\cos^2\theta \sin(\alpha - \beta)\sin(90^\circ + \theta + \delta - \alpha + \phi)} \right] \tag{4.12a}$$

where γ is unit weight of soil, parameters γ, ϕ, δ, θ, β, H are constants. α is a variable because BC is an assumed failure surface. P varies with α; the minimum of P represents the active earth pressure P_a, that is,

$$\frac{dP}{d\alpha} = 0 \tag{4.13}$$

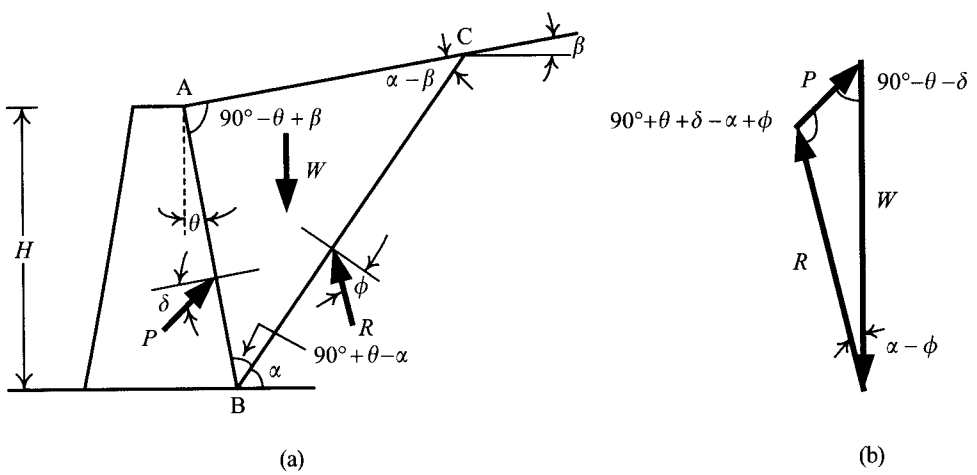

Figure 4.4 Coulomb's active earth pressure.

Substitute the critical α-value derived from the above equation in Eq. 4.12a and we will obtain the active earth pressure (P_a) as follows:

$$P_a = \tfrac{1}{2}\gamma H^2 K_a \tag{4.14}$$

$$K_a = \frac{\cos^2(\phi - \theta)}{\cos^2\theta\cos(\delta + \theta)\left[1 + \sqrt{\dfrac{\sin(\delta + \phi)\sin(\phi - \beta)}{\cos(\delta + \theta)\cos(\theta - \beta)}}\right]^2} \tag{4.14a}$$

where K_a is Coulomb's coefficient of active earth pressure. When $\theta = 0$, $\beta = 0$, and $\delta = 0$, $K_a = \tan^2(45° - \phi/2)$, which is identical with Rankine's.

Figure 4.5 illustrates passive soil failure in back of the retaining wall, which is pushed outward by an external force. BC in the figure is an assumed failure surface. The directions of the soil reaction force (R) and the reaction of the wall (P) are determined on the basis that the wall is pushed against soil and the wedge (ABC) moves upward. Following similar methods used in obtaining the active earth pressure, the passive earth pressure (P_p) can be derived and expressed by the following equation:

$$P_p = \tfrac{1}{2}\gamma H^2 K_p \tag{4.15}$$

$$K_p = \frac{\cos^2(\phi + \theta)}{\cos^2\theta\cos(\delta - \theta)\left[1 - \sqrt{\dfrac{\sin(\phi + \delta)\sin(\phi + \beta)}{\cos(\delta - \theta)\cos(\beta - \theta)}}\right]^2} \tag{4.15a}$$

where K_p is Coulomb's coefficient of passive earth pressure.

When $\theta = 0$, $\beta = 0$, and $\delta = 0$, Eq. 4.15a can be rewritten as $K_p = \tan^2(45° + \phi/2)$, which is identical with that of Rankine.

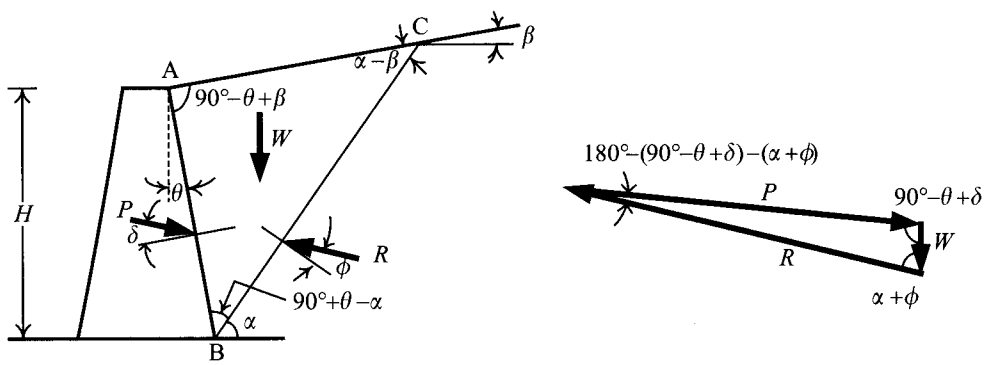

(a) (b)

Figure 4.5 Coulomb's passive earth pressure.

4.5 General discussion of various earth pressure theories

4.5.1 Displacement and earth pressure

According to the loading conditions of soil, when the soil's strained state changes from K_0 to active failure, the direction of its principal stresses will remain unchanged. From K_0 to passive failure, its direction will change by a rotation of 90°. That is, σ_1 is originally vertical ($\sigma_1 = \sigma_v$) and then changes to be horizontal ($\sigma_1 = \sigma_h$). Both the major and minor principal stresses rotate by 90°.

Thus, the strain for soil to come to passive failure is greater than that for it to reach active failure. As to problems concerning retaining walls, there have been many experiments that explore the relationships between wall displacement and earth pressure. Figure 4.6 and Table 4.1 are the synthetic results from experiments on rigid gravity walls provided by NAVFAC DM7.2 (1982). As shown in Table 4.1, the necessary wall displacement inducing passive conditions for cohesionless soils is four times larger than that inducing active conditions. For cohesive soils, the relationship is about two times.

Concerning problems of deep excavation, since the rigidity of the wall is much smaller than that of the gravity retaining wall, under the working load, displacement at the bottom of the wall (see Figure 4.7) may be too small to induce passive failure. Thus it is reasonable to infer that the actual earth pressure near the wall bottom is smaller than the passive earth pressure. However, the displacement of the retaining wall near the excavation surface is actually large enough to cause passive failure of soil in the vicinity of the excavation surface. Thus, the actual distribution of earth pressure on the passive side is as illustrated in Figure 4.7b. On the other hand, with the smaller displacement necessary to produce active failure, active failure may well occur in soil generally outside of the excavation area (Ou *et al.*, 1998).

4.5.2 Comparisons of Rankine's and Coulomb's earth pressure theories

As discussed in Section 4.4, the results obtained from Rankine's and Coulomb's earth pressure theories are identical under the same conditions (smooth wall surfaces, level grounds, and homogeneous cohesionless soils) though the two theories are quite differently based. As described in Section 4.3, Rankine's earth pressure theory is based on the principle of the plasticity equilibrium of the strained soil. That is to say, soil at any point within the failure zone (also called the wedge) is indiscriminately at failure and thereby there are infinite failure surfaces. On the other hand, Coulomb's theory is derived according to the principle of force equilibrium. As a result, there is only one failure surface, which is a plane, assuming that the wedge between the failure surface and the retaining wall is rigid.

The actual conditions, however, may not conform to the hypothetical terms: the wall surface may be rough and the ground surface in back of the wall may be of irregular shape with certain load. Rankine's theory can hardly apply under these conditions. Coulomb's theory can cope with these complicated conditions, though it is difficult to obtain a theoretical solution. Solutions to active and passive earth pressures, nevertheless, can be attained by Culmann's (1875) graphic method. Apparently, Coulomb's theory is more readily applicable. Practical cases, however, don't always work out that way. It depends on whether the hypotheses

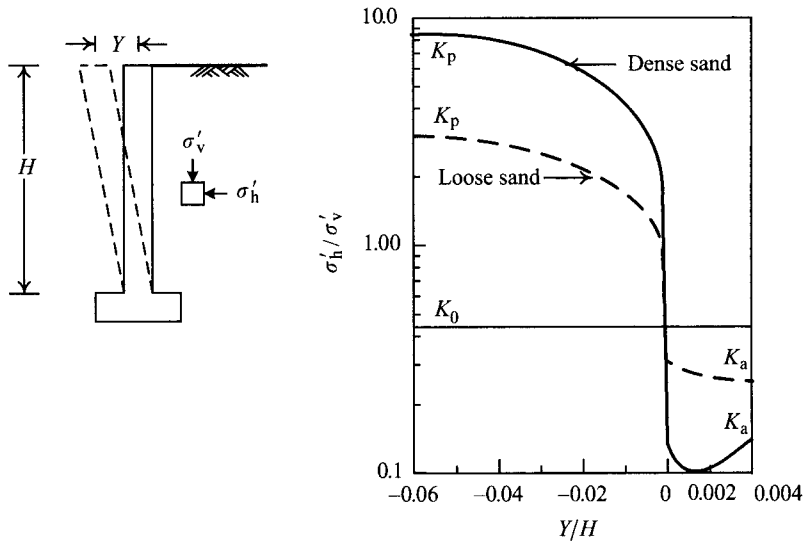

Figure 4.6 Effect of wall movement on earth pressure (Y is the lateral movement at the top of the wall and H is the wall height) (NAVFAC DM7.2, 1982).

Table 4.1 Magnitudes of wall rotation to reach failure (NAVFAC DM7.2, 1982)

Soil type	*Y/H*	
	Active	*Passive*
Dense cohesionless	0.0005	0.002
Loose cohesionless	0.002	0.006
Stiff cohesive	0.01	0.02
Soft cohesive	0.02	0.04

Note
Y is the movement at the wall top and H is the height of the wall (see Figure 4.6).

of Coulomb's earth pressure theory are in accordance with the field conditions, as will be discussed in the next section.

4.5.3 *Reliability of earth pressure theories and other solutions*

Whether Rankine's or Coulomb's earth pressure theories are reliable to represent the actual earth pressure depends on how close the hypotheses of the two theories are to the field condition. According to many studies and experiments (Peck and Ireland, 1961; Rowe and Peaker, 1965; Mackey and Kirk, 1967; James and Bransby, 1970; Rehnman and Broms, 1972), since

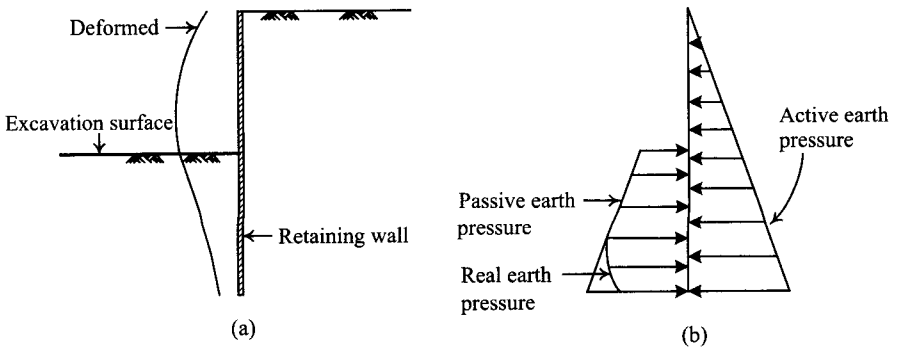

Figure 4.7 Excavation-induced deformation of a retaining wall and the distribution of lateral earth pressure: (a) wall deformation and (b) distribution of lateral earth pressure.

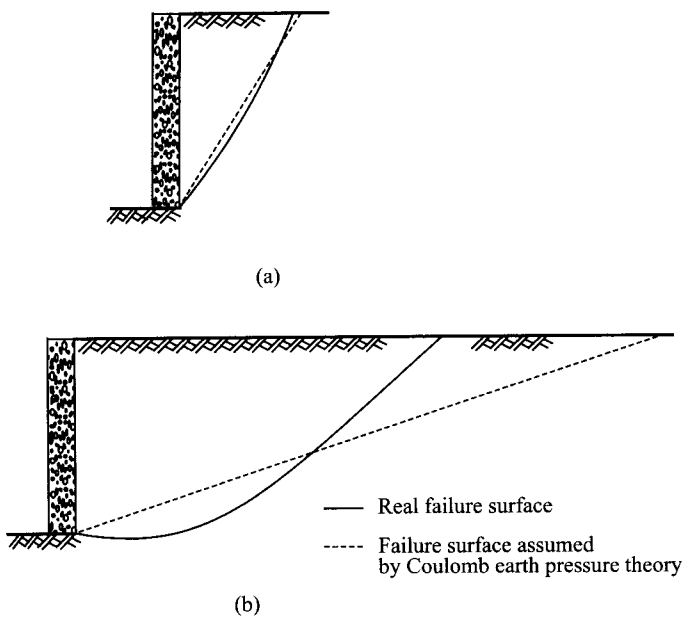

Figure 4.8 Real failure surfaces and failure surfaces assumed by Coulomb's earth pressure theory: (a) active condition and (b) passive condition.

there exists friction between retaining walls and soil, the failure surfaces of active failure and passive failure are both curved surfaces rather than planes. As Figure 4.8 shows, the actual active failure surface and Coulomb's assumed one are close. On the other hand, the actual passive failure surface can be rather different from that assumed by Coulomb's. The less the friction between the retaining wall and the surrounding soil, the closer the failure surface to a plane.

Many theories of active and passive earth pressure are developed on the assumption that the passive failure surface (as line segment BC in Figure 4.5a) is a curve function. For

example, Caquot and Kerisel (1948) assumed that it was an elliptical curved surface, James and Bransby (1970) assumed it to be a log spiral, Terzaghi and Peck (1967) assumed it to be another log spiral. Basically speaking, the better the assumed function of the curved surface represents the actual failure surface, the closer the derived earth pressure will be to the real earth pressure. None of the theories can be expressed in a simple equation. Among them, Caquot and Kerisel's assumed failure surface is quite close to the actual one and the derived coefficients of earth pressure are expressed by many tables to be readily applied. Thus, the coefficients of the active and passive earth pressures derived from the Coquot-Kerisel theory are seen to be very close to the real ones and are widely adopted in engineering practice (e.g. NAVFAC DM7.2, 1982; Padfield and Mair, 1984).

Figures 4.9 and 4.10 are, separately, the coefficients of the active and passive earth pressures induced from Rankine's, Coulomb's, and Caquot-Kerisel's theories on the assumptions of level ground and vertical walls (for the directions of P_a and P_a, see Figure 4.11). As shown in Figure 4.9, we can see when $\delta = 0$ (δ is the friction angle between the wall and the surrounding soil), the coefficients of active earth pressure obtained from Rankine's, Coulomb's, and Caquot-Kerisel's theories will be identical. When $\delta > 0$, the coefficient from Rankine's will come out the largest while Coulomb's and Caquot-Kerisel's will be close. The difference between Coulomb's coefficient of active earth pressure and Caquot-Kerisel's grows smaller and smaller with the decrease of δ. As we note, Caquot-Kerisel's coefficient of active earth pressure and Coulomb's will almost always come out identical when $\delta \leq 0.67\phi'$. In applications, K_a can be obtained, with δ and ϕ' known, by referring to Figure 4.9. The horizontal component of the earth pressure $\sigma_{a,h} = \gamma H K_{a,h} = \gamma H K_a \cos\delta$ and $P_{a,h} = (\gamma H^2 K_a \cos\delta)/2$ can then be computed accordingly.

From Figure 4.10, we can see that Rankine's, Coulomb's, and Caquot-Kerisel's coefficients of passive earth pressure are all the same, when $\delta = 0$. If $\delta > 0$, K_p, computed according to Rankine's earth pressure theory, will be the smallest, while that computed according to Coulomb's the largest. If $\phi' > 40°$, Coulomb's K_p will come out unreasonably large especially when $\delta = \phi'$. Observed from Figure 4.10, if $\delta \leq 0.5\phi'$, Coulomb's coefficient of passive earth pressure and Caquot-Kerisel's will be close. In applications, K_p can be obtained, with δ and ϕ' known, by referring to Figure 4.10. The horizontal component of the earth pressure $\sigma_{p,h} = \gamma H K_{p,h} = \gamma H K_p \cos\delta$ and $P_{p,h} = (\gamma H^2 K_p \cos\delta)/2$ can then be computed accordingly.

For problems of excavation, considering that the active earth pressure is usually the main force leading to the failure of retaining walls, Caquot-Kerisel's active earth pressure should be adopted for analysis and design since it is regarded as most close to the real active earth pressure. Slightly smaller than Caquot-Kerisel's, almost the same under most circumstances, Coulomb's coefficient of active earth pressure is also workable for analysis and design. For conservative reasons, Rankine's coefficient of active earth pressure is recommended for it is the largest among the three without significant difference from Caquot-Kerisel's.

The passive earth pressure is usually the force resisting failure. Caquot-Kerisel's passive earth pressure is regarded as the real passive earth pressure and is therefore the most favored choice. Rankine's coefficient of passive earth pressure deviates much from the real value, usually too small, to be applicable. When $\delta < 0.5\phi'$, Coulomb's does not differ significantly from Caquot-Kerisel's and is workable. On the other hand, when $\delta \geq 0.5\phi'$, it is so much larger than Caquot-Kerisel's that it is unsafe to adopt for analysis and design.

As to related problems of analysis and design, please see Chapter 5.

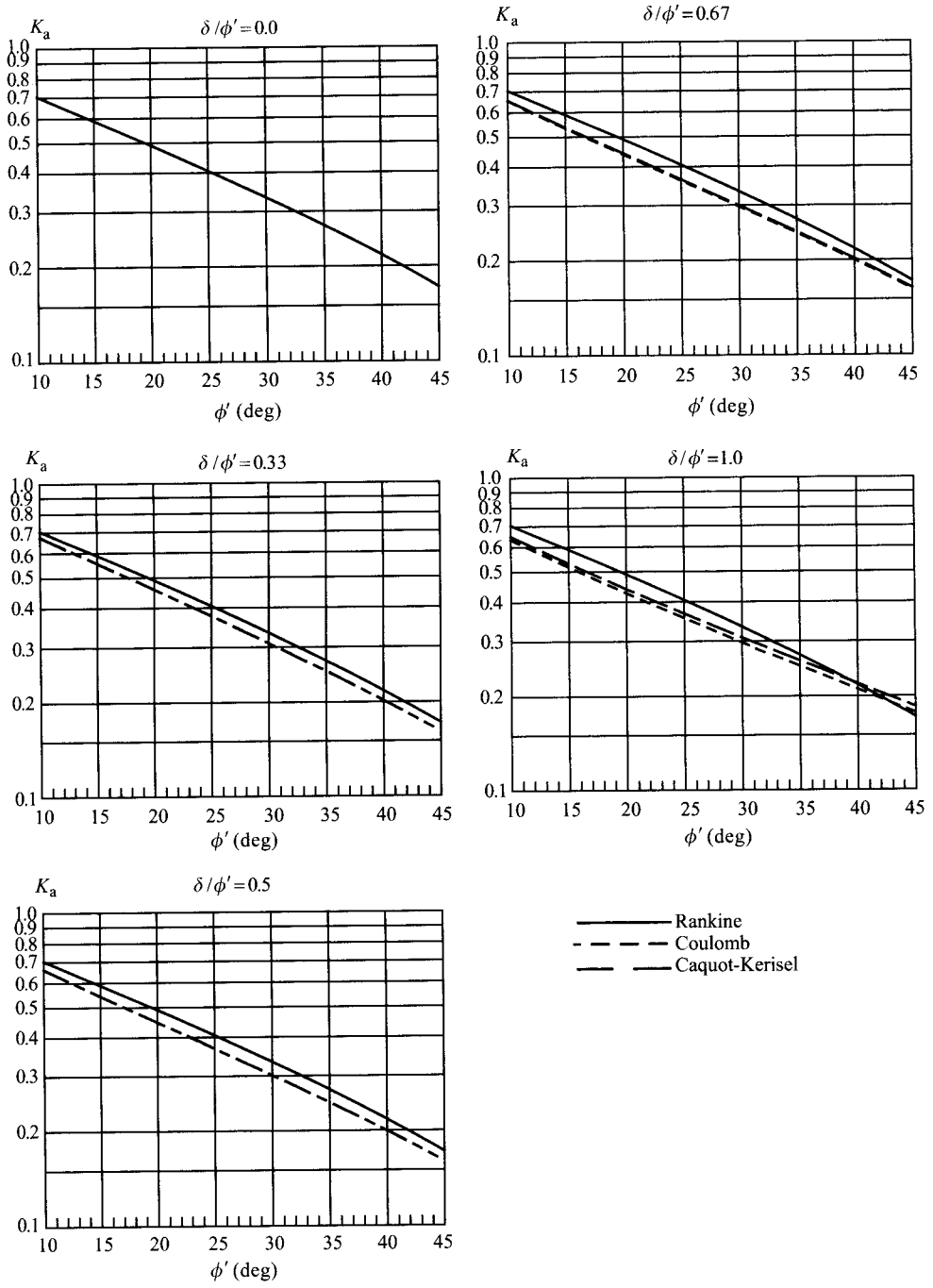

Figure 4.9 Coefficients of Rankine's, Coulomb's, and Caquot-Kerisel's active earth pressure (horizontal component $K_{a,h} = K_a \cos \delta$).

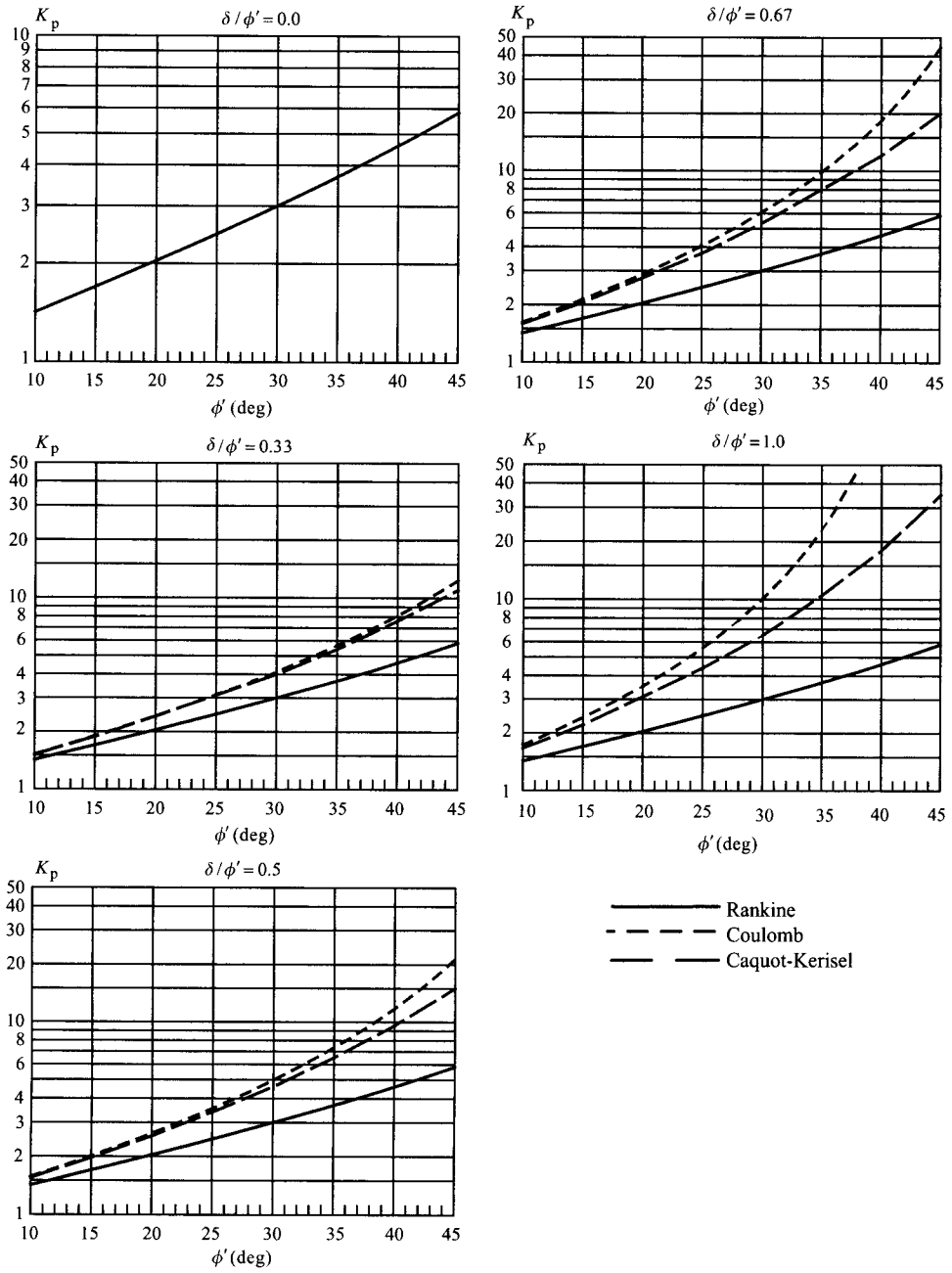

Figure 4.10 Coefficients of Rankine's, Coulomb's, and Caquot-Kerisel's passive earth pressure (horizontal component $K_{p,h} = K_p \cos \delta$).

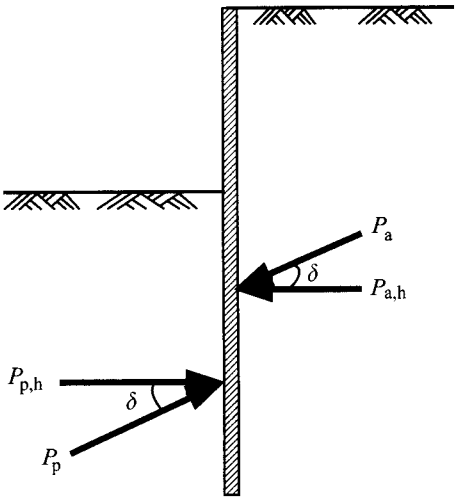

Figure 4.11 Active and passive forces of level cohesionless soils on a vertical wall.

4.6 Earth pressure for design

Theoretically speaking, Rankine's earth pressure can be applied both to cohesive and cohesionless soils. Nevertheless, it is unable to consider the adhesion or friction between retaining walls and soil. On the other hand, Coulomb's and Caquot-Kerisel's earth pressure can take into consideration the friction between retaining walls and soil, though they can only apply to cohesionless soils. Following Padfield and Mair's (1984) suggestion, this section will adopt Rankine's earth pressure theory and Caquot-Kerisel's coefficient of earth pressure together to calculate earth pressure for problems of deep excavation. Though the section mainly focuses on deep excavations, the methods are generally applicable to other problems of geotechnical engineering.

4.6.1 Cohesive soils

As to the short-term behavior of cohesive soils, their earth pressures should be obtained following the total stress method while the parameters of soil strength should be derived from the UU test, the FV test, or the CPT test. If the cohesive soil is 100% saturated, it should be analyzed assuming $\phi = 0$. Considering the adhesion between retaining walls and soil (i.e. the surface of the retaining wall is not smooth), the earth pressures for design can be expressed as follows (Padfield and Mair, 1984):

$$\sigma_a = \sigma_v K_a - 2cK_{ac} \tag{4.16}$$

$$K_{ac} = \sqrt{K_a\left(1 + \frac{c_w}{c}\right)} \tag{4.17}$$

$$\sigma_p = \sigma_v K_p + 2cK_{pc} \tag{4.18}$$

$$K_{pc} = \sqrt{K_p\left(1 + \frac{c_w}{c}\right)} \tag{4.19}$$

where

σ_a = total active earth pressure (horizontal) acting on the retaining wall
σ_p = total passive earth pressure (horizontal) acting on the retaining wall
c = cohesion intercept
ϕ = angle of friction, based on the total stress representation
c_w = adhesion between the retaining wall and soil
K_a = coefficient of active earth pressure
K_p = coefficient of passive earth pressure.

When cohesive soils are completely saturated, $\phi = 0$ and c equals the undrained shear strength s_u; that is, $K_a = K_p = 1$, $K_{ac} = K_{pc} = \sqrt{1 + c_w/s_u}$ where the value of c_w can be estimated by the following equation:

$$c_w = \alpha s_u \tag{4.20}$$

where α is a reduction factor, which relates to the soil strength, the construction method of the retaining wall, and the roughness of its surface.

Adhesion between the retaining wall (note: for excavation) and the surrounding soil is not well studied. There exist, nevertheless, many studies on adhesion between pile foundations and soil. Striking and casting in situ are two common construction methods for pile foundations. The pile material can be steel or concrete, etc. Thus, it may be feasible to apply the studies on pile foundations to retaining walls for deep excavations. The suggested relations between α and s_u/σ_v' by API (the American Petroleum Institute, 1993) and the study results of bored piles in Taipei (Lin and Lin, 1999) are shown in Figure 4.12, and can be used to estimate the α-value.

According to Eqs 4.16 and 4.18, the distribution of earth pressures in front of and in back of the retaining wall should be similar to Figure 4.3a, where the resultants of $\sigma_a$and σ_p are all perpendicular to the retaining wall (referring to the conditions where the ground is level). From Figure 4.3a, we can see that there exists a tension zone in the cohesive soils in back of the wall. A tension crack will occur if the soil is subject to long-term tensile stress. The depth of a tension crack can be estimated by Eq. 4.16 with $c_w = 0$. Let the lateral earth pressure be 0, then

$$\sigma_a = \gamma z K_a - 2c\sqrt{K_a} = 0 \tag{4.21}$$

The depth of a tension crack is

$$z_c = \frac{2c}{\gamma\sqrt{K_a}} \tag{4.22}$$

where z_c = depth of a tension crack.

Once tension cracks are produced, the soils are no longer able to bear tensile stress. Thus, to be conservative, we often suppose that there already exist tension cracks in the design. Rain and environmental factors will further make cracks full of moisture, so that they begin to push

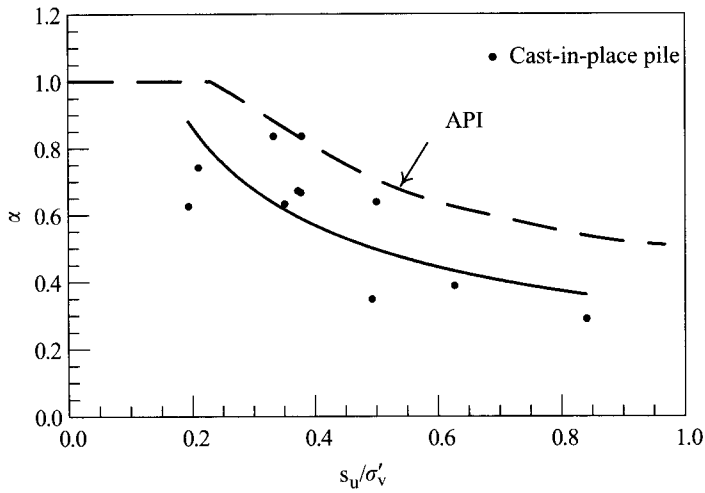

Figure 4.12 Relation between adhesion and undrained shear strength of clay.

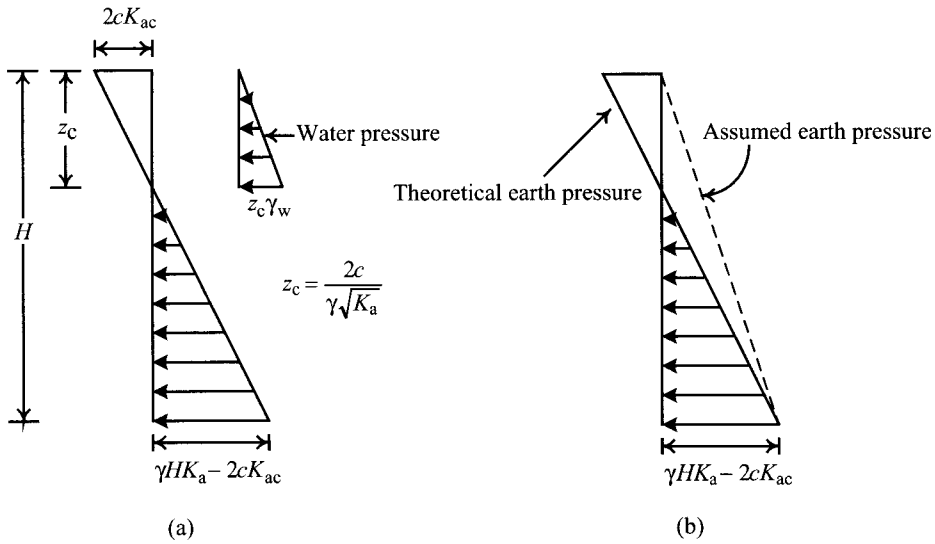

Figure 4.13 Distribution of lateral earth pressure for the cohesive soil.

the retaining wall as shown in Figure 4.13a. For problems of deep excavation, considering the possibilities that soil creep in the tension zone may lead more soil to jostle against the retaining wall, the distribution of earth pressure may be as illustrated in Figure 4.13b.

The long-term behavior of cohesive soils should be analyzed on the basis of the complete dissipation of the excess porewater pressure. The distribution of earth pressure is to be estimated the same way as that of cohesionless soils, as will be discussed in the following section.

4.6.2 Cohesionless soils

The excess porewater pressure of cohesionless soils dissipates quickly as soon as shearing occurs. As a result, the analysis should follow the effective stress method. Supposing there exists friction between the retaining wall and the surrounding soil, the earth pressure for design can be represented as follows (Padfield and Mair, 1984):

$$\sigma'_a = K_a(\sigma_v - u) - 2c'K_{ac} \tag{4.23}$$

$$K_{ac} = \sqrt{K_a\left(1 + \frac{c'_w}{c'}\right)} \tag{4.24}$$

$$\sigma_a = \sigma'_a + u \tag{4.25}$$

$$\sigma'_p = K_p(\sigma_v - u) + 2c'K_{pc} \tag{4.26}$$

$$K_{pc} = \sqrt{K_p\left(1 + \frac{c'_w}{c'}\right)} \tag{4.27}$$

$$\sigma_p = \sigma'_p + u \tag{4.28}$$

where

σ'_a = effective active earth pressure acting on the retaining wall
σ'_p = effective passive earth pressure acting on the retaining wall
σ_a = total active earth pressure
σ_p = total passive earth pressure
K_a = Caquot-Kerisel's coefficient of active earth pressure
K_p = Caquot-Kerisel's coefficient of passive earth pressure
c' = effective cohesion intercept
ϕ' = effective angle of friction
c_w = effective adhesion between the retaining wall and soil
u = porewater pressure.

For most cohesionless soils, $c' = 0$, $c'_w = 0$; therefore, $K_{ac} = K_a$, $K_{pc} = K_p$. K_a and K_p can be determined referring to Figures 4.9 and 4.10, given the values of ϕ' and δ. To obtain the horizontal component of active earth pressure ($\sigma_{a,h}$), $K_{a,h}$ should substitute for K_a in Eqs 4.23–4.25 and $K_{p,h}$ should substitute for K_p in Eqs 4.26–4.28 to obtain the horizontal component of passive earth pressure ($\sigma_{p,h}$), where $K_{a,h} = K_a \cos\delta$ and $K_{p,h} = K_p \cos\delta$.

Clough (1969) studied the characteristics of friction between concrete and sand using the direct shear test and found that the friction angle (δ) between concrete and sand is around $0.83\phi'$ (where ϕ' stands for the friction angle of sand). Potyondy (1961) employed a smooth steel mold to cast concrete, which was in turn employed to explore the characteristics of friction between concrete and sand by tests, and found $\delta = 0.8\phi'$. Chapter 5 will explore further reasonable friction angles (δ) between retaining walls and soils.

A tension zone or a tension crack zone will not occur in cohesionless soils because $c' = 0$. Sometimes a value of c' may be found which is other than 0 in design, the reason for which might be that c' is an apparent earth pressure or a deviation due to regression analysis of test results. Whichever is the case, there cannot exist a tension zone or a tension crack zone in cohesionless soils and some necessary modifications are required.

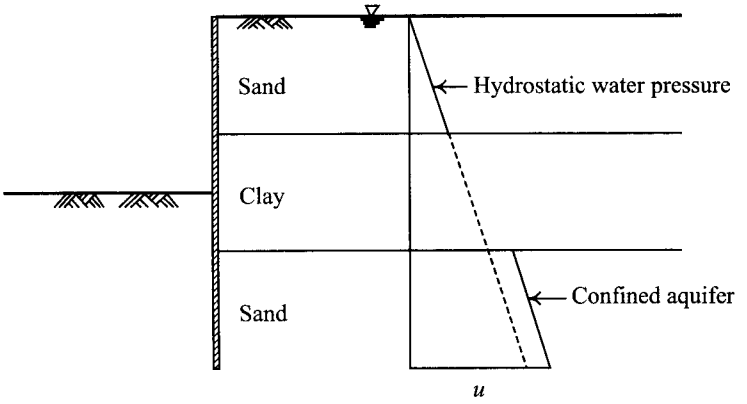

Figure 4.14 Distribution of water pressures for alternated layers.

4.6.3 Alternated layers

To compute the distribution of earth pressures for alternated layers composed of both cohesive and cohesionless soils, the total stress analysis should be adopted for (short-term behavior of) cohesive soils, the water pressure will not be considered while doing the effective stress analysis for cohesionless soils, the water pressure is to be computed separately. Note that cohesive soils do not necessarily have static water pressure because of the influences of geology formation, the environment change, and past dewatering history. If working with the long-term behavior, the effective stress analysis should be applied to both cohesive and cohesionless soils and the water pressure should be computed separately. Figure 4.14 illustrated a typical formation of alternated and a "possible" distribution of porewater pressure.

4.6.4 Sloping ground

According to Rankine's earth pressure theory, the coefficients of the earth pressure for sloping ground (Bowles, 1988) can be computed as follows:

$$K_a = \cos\beta \frac{\cos\beta - \sqrt{\cos^2\beta - \cos^2\phi}}{\cos\beta + \sqrt{\cos^2\beta - \cos^2\phi}} \tag{4.29}$$

$$K_p = \cos\beta \frac{\cos\beta + \sqrt{\cos^2\beta - \cos^2\phi}}{\cos\beta - \sqrt{\cos^2\beta - \cos^2\phi}} \tag{4.30}$$

where ϕ is the angle of friction and β is the slope of the ground.

Thus, the active and passive earth pressures, and their resultants acting on the retaining wall as shown in Figure 4.15 are:

$$\sigma_a = \gamma z K_a \tag{4.31}$$

$$P_a = \tfrac{1}{2}\gamma H^2 K_a \tag{4.32}$$

$$\sigma_p = \gamma z K_p \tag{4.33}$$

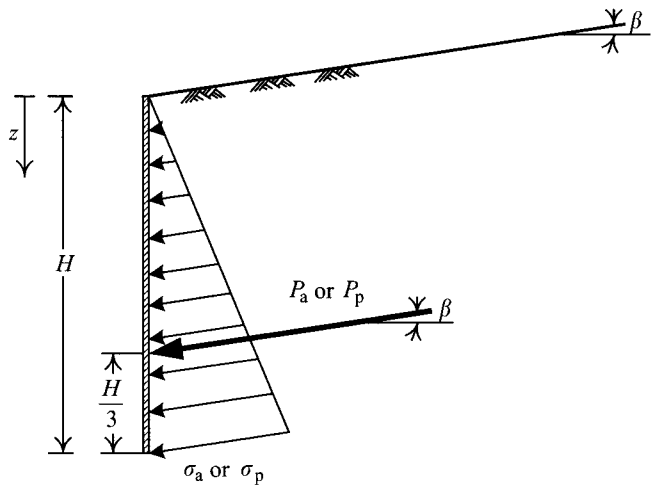

Figure 4.15 Earth pressure for sloping ground.

$$P_p = \tfrac{1}{2}\gamma H^2 K_p \tag{4.34}$$

where

γ = unit weight of soil
H = height of the retaining wall
σ_a = active earth pressure
σ_p = passive earth pressure
P_a = resultant of active earth pressure
P_p = resultant of passive earth pressure.

In problems of deep excavation, only the horizontal components are relevant and they are:

$$\sigma_{a,h} = \gamma z K_a \cos\beta \tag{4.35}$$

$$P_{a,h} = \frac{1}{2}\gamma H^2 K_a \cos\beta \tag{4.36}$$

$$\sigma_{p,h} = \gamma z K_p \cos\beta \tag{4.37}$$

$$P_{p,h} = \frac{1}{2}\gamma H^2 K_p \cos\beta \tag{4.38}$$

Figure 4.16 shows the comparison of coefficients of horizontal active earth pressure derived from Rankine's, Coulomb's, and Caquot-Kerisel's earth pressure theories for the conditions of $\beta/\phi' = 1.0$ and $\delta/\phi' = 1.0$. As shown in the figure, the coefficients of Rankine's earth pressure come out the largest and those of Coulomb's and Caquot-Kerisel's theories are almost identical. Apparently, the active earth pressure on the back of the retaining wall can be computed by Eq. 4.14, that is, Coulomb's earth pressure theory. Inside the excavation zone the ground is mostly level, so the passive earth pressure can be obtained from Caquot-Kerisel's

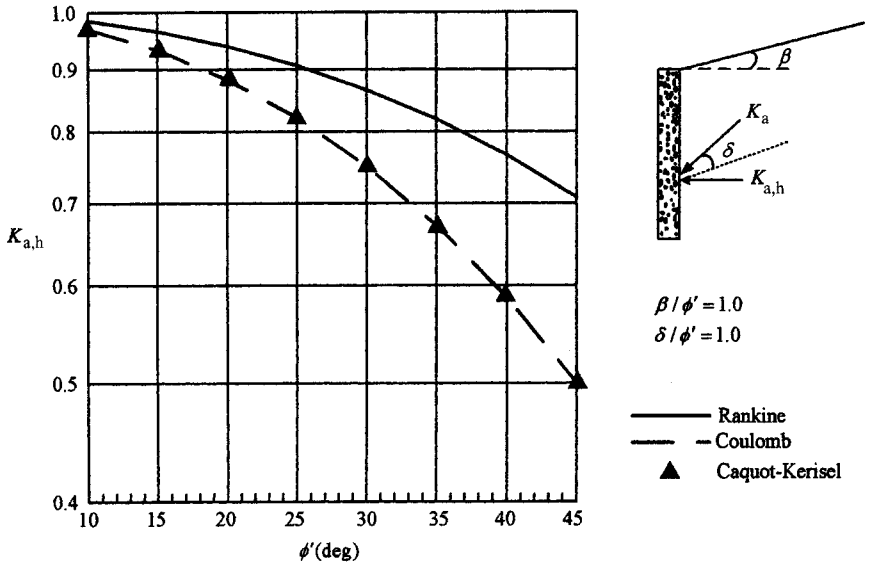

Figure 4.16 Coefficients of Rankine's, Coulomb's, and Caquot-Kerisel's horizontal active earth pressure.

earth pressure theory as Figure 4.10 shows (see Section 4.5.3). Besides, NAVFAC DM 7.2 also provides the passive earth pressure of a sloping ground according to Caquot-Kerisel's earth pressure theory. Seldom confronted in deep excavation, the question will not be further discussed here.

4.6.5 Surcharge

As shown in Figure 4.17, the uniformly distributed load, q, extensively acts on the ground surface while p acts on the excavation bottom. The load-induced active and passive earth pressures on the retaining wall are separately:

$$\sigma_a = qK_a \tag{4.39}$$

$$\sigma_p = pK_p \tag{4.40}$$

where

K_a = Caquot-Kerisel's coefficient of active earth pressure, which can be determined by referring to Figure 4.9,
K_p = Caquot-Kerisel's coefficient of passive earth pressure, which can be determined by referring to Figure 4.10.

If the load is neither uniformly nor extensively distributed, the thrust of load against the wall will then be a problem of the theory of elasticity. According to Gerber (1929) and

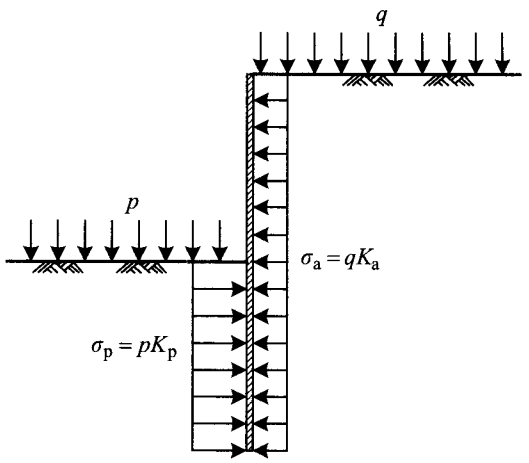

Figure 4.17 Lateral earth pressure produced by uniformly distributed load.

Spangler (1938), the distribution of earth pressure (σ_h) against the wall caused by a point load Q_p can be expressed in m, n as follows:

$$m \leq 0.4$$

$$\sigma_h = \frac{0.28Q_p}{H^2}\frac{n^2}{(0.16+n^2)^3} \tag{4.41}$$

$$m > 0.4$$

$$\sigma_h = \frac{1.77Q_p}{H^2}\frac{m^2n^2}{(m^2+n^2)^3} \tag{4.42}$$

Figure 4.18a illustrates the dimensionless diagram of earth pressure distribution derived from the above equation where m is separately made 0.2, 0.4, and 0.6. The corresponding resultant of earth pressure (P_h) and the point of action R are marked in the figure. Figure 4.18c is the diagram of the earth pressure (σ_h) at depth z below the ground surface (the AA section in Figure 4.18a) where $\sigma_{h,\theta}$ is

$$\sigma_{h,\theta} = \sigma_h \cos^2(1.1\theta) \tag{4.43}$$

Figure 4.19a illustrates the earth pressure distribution caused by a line load paralleling the retaining wall (Q_ℓ), whose earth pressure and earth pressure resultant can be expressed as follows:

$$m \leq 0.4$$

$$\sigma_h = \frac{0.203Q_\ell}{H}\frac{n}{(0.16+n^2)^2} \tag{4.44}$$

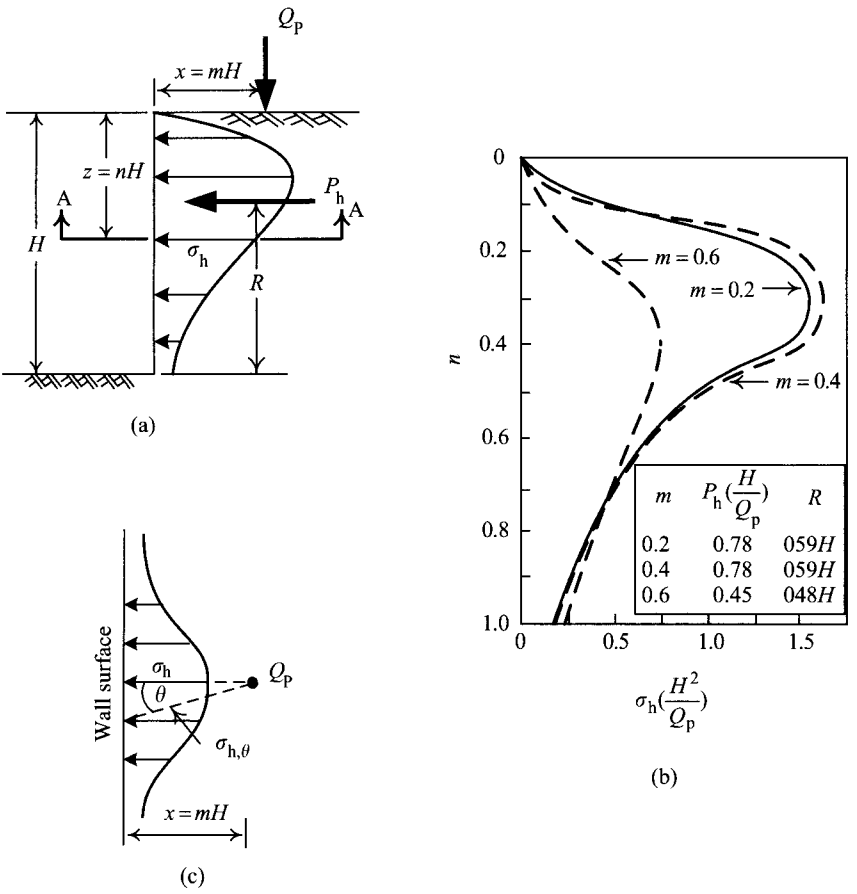

Figure 4.18 Lateral earth pressure produced by a point load Q_p: (a) notations, (b) vertical profile of lateral stress distribution, and (c) horizontal profile of lateral stress distribution.

$m > 0.4$

$$\sigma_h = \frac{1.28Q_\ell}{H}\frac{m^2 n}{(m^2+n^2)^2} \tag{4.45}$$

and their resultant is

$$P_h = \frac{0.64Q_\ell}{(m^2+1)} \tag{4.46}$$

Figure 4.19b illustrates the dimensionless diagram of earth pressure distribution derived from the above equation where m is separately made 0.1, 0.3, 0.5, and 0.7. The corresponding point of action R is also marked in the figure.

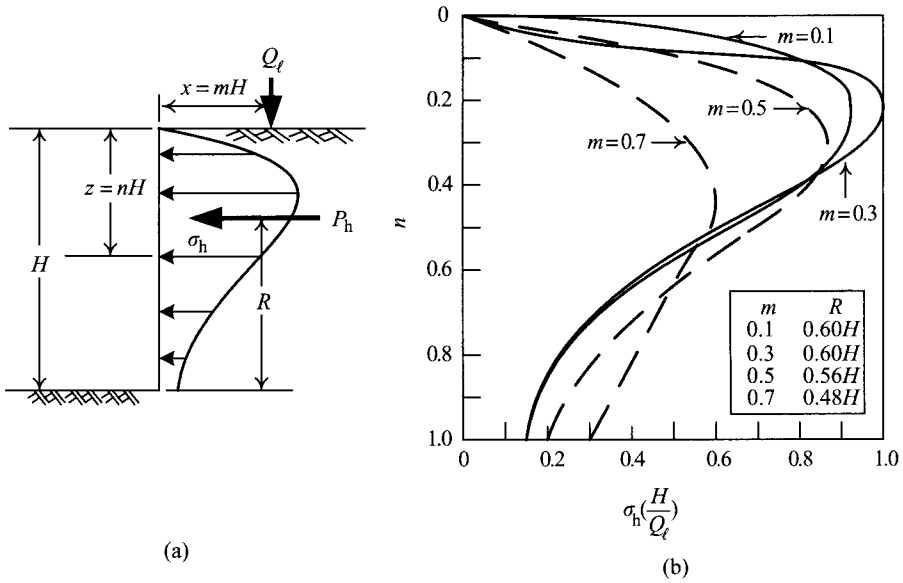

Figure 4.19 Lateral earth pressure produced by a line load Q_ℓ: (a) notations and (b) vertical profile of lateral stress distribution.

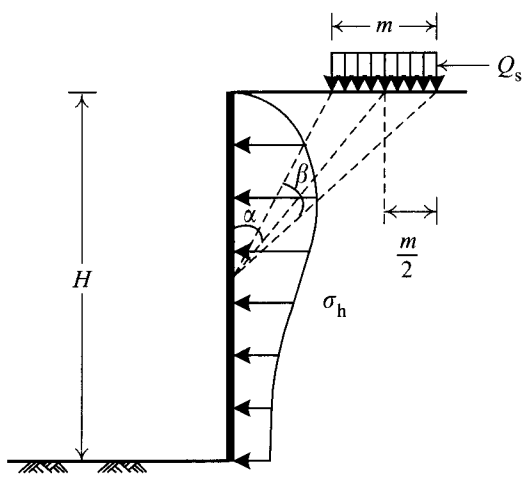

Figure 4.20 Lateral earth pressure produced by a strip load Q_s.

Figure 4.20 illustrates a strip load (Q_s) paralleling the retaining wall. According to the theory of elasticity, the lateral earth pressure (σ_h) at depth z is

$$\sigma_h = \frac{Q_s}{H}(\beta - \sin\beta\cos 2\alpha) \tag{4.47}$$

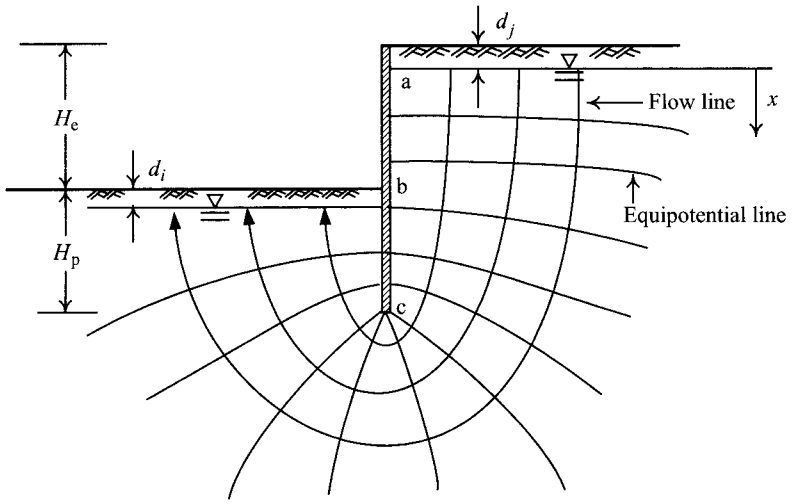

Figure 4.21 Seepage in an excavation zone.

Considering the restraining effect of the retaining wall, the earth pressure acting on the wall can be modified from Eq. 4.47 to the following:

$$\sigma_h = \frac{2Q_s}{H}(\beta - \sin\beta\cos 2\alpha) \tag{4.48}$$

4.6.6 Seepage

Cohesionless soils have a high degree of permeability. As a result, the difference of the water levels between the excavation bottom and the area outside the excavation in cohesionless soils will cause seepage. Cohesive soils exhibit undrained behavior in the short-term condition. That is to say, no seepage is to be considered. In the long run, cohesive soils may also produce seepage and can be analyzed in the same way as cohesionless soils.

Seepage will affect the water pressures inside and outside the excavation zone and also the effective stresses. In deep excavations, seepage caused by the difference of water level is two-dimensional and the corresponding variation of water pressure can be estimated by flow net or using the finite element method. Figure 4.21 is a typical diagram of the flow net.

Generally speaking, excavation will encounter various soil layers. The subsurface soil may not be homogeneous or isotropic. Considering the difficulty of the depiction of a non-homogeneous and non-isotropic flow net, for the sake of simplification, we sometimes assume that the behavior of seepage is one dimensional, that is, the head loss per unit length of a flow path is the same.

As shown in Figure 4.22a, the difference of the total heads between the upstream water level (outside the excavation zone) and the downstream water level is $(H_e + d_i - d_j)$. The length of the path of the water flowing from the upstream water level along the retaining wall down to the downstream water level is $(2H_p + H_e - d_i - d_j)$. Assuming that the datum of the elevation

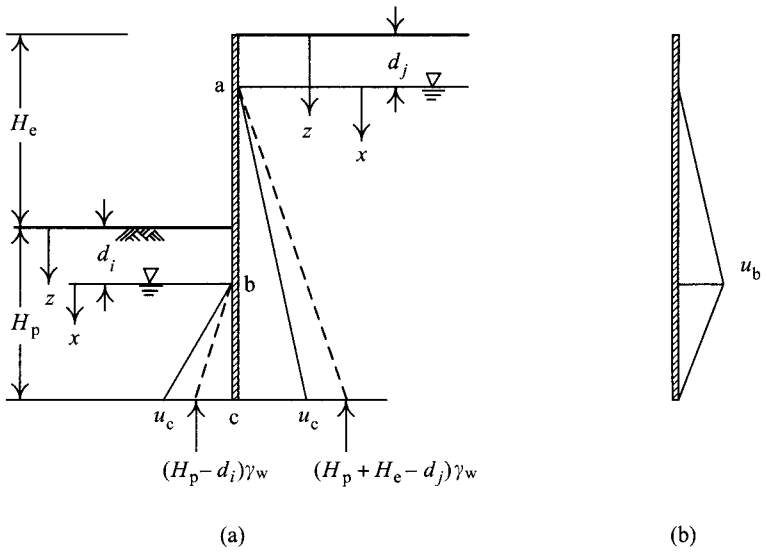

Figure 4.22 Simplified analysis method for seepage: (a) distribution of water pressure and (b) net water pressure.

head is set to be the same with the upstream water level, the total head (h) at a distance of x from the upstream water level would be:

$$h = 0 - \frac{x(H_e + d_i - d_j)}{2H_p + H_e - d_i - d_j} = -\frac{x(H_e + d_i - d_j)}{2H_p + H_e - d_i - d_j} \tag{4.49}$$

Let h_e be the elevation head and h_p the pressure head. The pressure head at a distance of x from the upstream water level would be:

$$h_p = h - h_e = \frac{-x(H_e + d_i - d_j)}{2H_p + H_e - d_i - d_j} - (-x) = \frac{2x(H_p - d_i)}{2H_p + H_e - d_i - d_j} \tag{4.50}$$

Thus, the water pressure, u_x, at a distance of x from the upstream water level would be:

$$u_x = \frac{2x(H_p - d_i)\gamma_w}{2H_p + H_e - d_i - d_j} \tag{4.51}$$

The water pressure at the bottom of the retaining wall, u_c, would be:

$$u_c = \frac{2(H_p + H_e - d_j)(H_p - d_i)\gamma_w}{2H_p + H_e - d_i - d_j} \tag{4.52}$$

When actually conducting an excavation analysis, the distribution of water pressure is usually expressed in the net water pressure (please see Section 5.5). The largest net water pressure is to be found at b, whose value would be:

$$u_b = \frac{2(H_e + d_i - d_j)(H_p - d_i)\gamma_w}{2H_p + H_e - d_i - d_j} \tag{4.53}$$

As shown in Figure 4.22a, seepage will decrease the porewater pressure on the active side (lower than the hydrostatic water pressure) and increase it on the passive side (higher than the hydrostatic water pressure). As discussed earlier, we can derive the rates of increase of porewater pressure per unit length on the active and passive sides as follows:

$$\mu_a = \frac{u_c}{H_p + H_e - d_j} \tag{4.54}$$

$$\mu_p = \frac{u_c}{H_p - d_i} \tag{4.55}$$

where μ_a and μ_p represent the rates of increase of the porewater pressure per unit length on the active and passive sides, respectively.

Thus, the water pressures x below the water level at the active and passive sides are separately $u_x = \mu_a x$ (the active side) and $u_x = \mu_p x$ (the passive side).

Therefore, μ_a and μ_p can be seen as the modified unit weights of water on the active side and passive side, respectively. As a result, the total lateral earth pressure at a depth of z below the ground surface on the back of the wall would be:

$$\sigma_h = \sigma'_v K_a + u \tag{4.56}$$

$$= \left[\sigma_v - \frac{(z - d_j)}{H_p + H_e - d_j} u_c\right] K_a + \frac{(z - d_j)}{H_p + H_e - d_j} u_c \tag{4.57}$$

Similarly, the total lateral earth pressure at a distance of z below the ground surface on the front of the wall would be:

$$\sigma_h = \sigma'_v K_p + u \tag{4.58}$$

$$= \left[\sigma_v - \frac{(z - d_i)}{H_p - d_i} u_c\right] K_p + \frac{(z - d_i)}{H_p - d_i} u_c \tag{4.59}$$

4.6.7 Earthquakes

Earthquakes will engender lateral and vertical acceleration, which will in turn increase the active earth pressure outside the retaining wall and decrease the passive earth pressure inside the wall. The Mononobe–Okabe equation is generally adopted (Okabe, 1926; Mononobe, 1929) to compute the active and passive earth pressures under the influence of earthquakes. As shown in Figure 4.23, the active and passive earth pressures (P_{ae}, P_{pe}) under the influence of earthquakes can be computed by the following equations:

$$P_{ae} = \frac{1}{2}\gamma H_1^2 (1 - k_v) K_a \tag{4.60}$$

$$K_a = \frac{\cos^2(\phi - \alpha_a - \theta)}{\cos\theta \cos^2\alpha_a \cos(\delta + \alpha_a + \theta)\left\{1 + \left[\frac{\sin(\phi + \delta)\sin(\phi - \beta_a - \theta)}{\cos(\delta + \alpha_a + \theta)\cos(\beta_a - \alpha_a)}\right]^{1/2}\right\}^2} \tag{4.61}$$

$$P_{pe} = \frac{1}{2}\gamma H_2^2 (1 - k_v) K_p \tag{4.62}$$

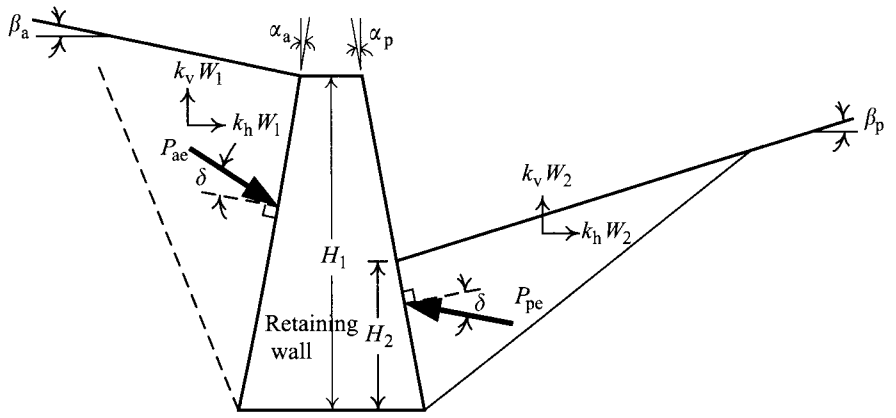

W_1: Weight of wedge in the active zone

W_2: Weight of wedge in the passive zone

Figure 4.23 Active and passive earth pressure under the influence of earthquakes.

$$K_p = \frac{\cos^2(\phi + \alpha_p - \theta)}{\cos\theta \cos^2\alpha_p \cos(\delta - \alpha_p + \theta)\left\{1 - \left[\frac{\sin(\phi + \delta)\sin(\phi + \beta_p - \theta)}{\cos(\delta - \alpha_p + \theta)\cos(\beta_p - \alpha_p)}\right]^{1/2}\right\}^2} \tag{4.63}$$

where $\theta = \tan^{-1}[k_h/(1 - k_v)]$; k_h and k_v are the horizontal and vertical coefficients of earthquake, which are defined as follows:

$$k_h = \frac{\text{the horizontal acceleration of earthquake } (a_h)}{\text{the acceleration of gravity } (g)} \tag{4.64}$$

$$k_v = \frac{\text{the vertical acceleration of earthquake } (a_v)}{\text{the acceleration of gravity } (g)} \tag{4.65}$$

Some building codes have suggested that the horizontal coefficient of earthquake (k_h) for design be half of the horizontal peak acceleration of the site. With lateral displacement restrained, nevertheless, the dynamic earth pressure caused by an earthquake will be greater than the displacement without restraint. With the lateral displacement completely restrained, k_h can be estimated as 1.5 times as great as the horizontal peak acceleration of the site. The vertical coefficient of earthquake (k_v) for design can be assumed to be half of the vertical acceleration of the earthquake at the site. As for earthquakes occurring far away, however, the influence of vertical earthquake can be reasonably ignored, that is, $k_v = 0$. The peak acceleration of the site should be determined on the basis of design criteria of service life and risk analysis.

Location of action of the dynamic active pressure on the retaining wall depends on the type of the earthquake-induced displacement of the wall. There are three types of displacement

of a retaining wall: overturning about the wall toe, sliding along the wall base and rotating about the wall top. The first type, however, is the only one generally considered.

According to the characteristics of the earth pressure distribution, the static active and passive earth pressures act at distances of $H_1/3$ and $H_2/3$ from the base of the wall, respectively. The increment of active earth pressure ($P_{ae} - P_a$) and that of passive earth pressure ($P_{pe} - P_p$) due to earthquake act at distances of $2H_1/3$ and $2H_2/3$ from the base of the wall, respectively.

Besides, based on many tests, Bowles (1988) suggested that δ be assumed to be 0 in the dynamic condition.

If the wall rotates about the wall toe when earthquakes occur, the location of the dynamic active earth pressure resultant can be determined as follows:

1 Compute the increment of the active earth force ΔP_{ae}:

$$\Delta P_{ae} = P_{ae} - P_a \tag{4.66}$$

2 Locate P_a at a distance of $H_1/3$ from the base of the wall.
3 Locate ΔP_{ae} at a distance of $2H_1/3$ from the base of the wall.
4 Compute the location of P_{ae}, resultant of P_e and ΔP_{ae}:

$$\bar{z} = \frac{P_a(H/3) + \Delta P_{ae}(2H/3)}{P_{ae}} \tag{4.67}$$

The location of the dynamic passive earth pressure resultant can be determined similarly.

In design, the influence of earthquakes on the safety of a retaining wall as a permanent structure should be considered. In deep excavations, the outer walls of a basement are permanent structures. The design should thereby take into consideration the influence of earthquakes. If the diaphragm walls also serve as the outer walls of a basement, the influence of earthquakes should be considered accordingly. Otherwise, the influence of earthquakes can be ignored. As for temporary retaining structures such as soldier piles, steel sheet piles, and column piles, earthquake effects are ignorable.

4.7 Summary and general comments

The chapter can be summarized as follows:

1 For those retaining walls to which displacement does not occur, such as the outer wall of a basement, the lateral earth pressure at rest is to be adopted for design. The coefficients of at-rest lateral earth pressure for normally consolidated cohesive soils and cohesionless soils can be estimated by Jaky's equation. For overconsolidated soils, though some empirical equations for the coefficients of at-rest lateral earth pressure are also available, in situ tests are preferable.
2 Rankine's earth pressure theory cannot consider friction or adhesion between the retaining wall and soil. Coulomb's earth pressure theory, on the other hand, can. Though the two theories are differently based, the obtained earth pressures are the same when both assume a vertical and smooth wall back. Both theories assume the failure surfaces as planes, not conforming to reality, and thereby their results cannot represent real earth pressures.

3 Friction between the retaining wall and soil considered, failure surfaces are curved surfaces. Thus, Rankine's active earth pressure would overestimate the real earth pressure very slightly whereas its passive earth pressure would underestimate the real value. Caquot-Kerisel's earth pressures, both the active and the passive ones, are the closest to the real values and are regarded as the real earth pressures.

4 In problems of excavation, the active earth pressure is the main force engendering failure. Caquot-Kerisel's active earth pressure, regarded as the real earth pressure, is to be adopted for design. Coulomb's active earth pressure is smaller than Caquot-Kerisel's, but the difference is insignificant. Therefore, Coulomb's active earth pressure can be used for design, too. To be conservative, Rankine's active earth pressure is to be recommended for it is the largest among the three and does not differ significantly from Caquot-Kerisel's.

5 The passive earth pressure is often the force to resist failure. Caqout-Kerisel's earth pressure is the first choice for analysis and design since it is regarded as the real earth pressure. Rankine's earth pressure is too small and differs significantly from the real value. Thus, Rankine's is not to be adopted. When $\delta \leq 0.5\phi'$, Coulomb's coefficient of passive earth pressure is similar to that of Caqout-Kerisel's and is also feasible for analysis and design. When $\delta > 0.5\phi'$, on the other hand, Coulomb's coefficient of passive earth pressure is obviously larger than Caqout-Kerisel's and will render the design unsafe.

6 Seepage will decrease the water pressure on the active side and increase it on the passive side, and will in turn affect the effective stress and the lateral earth pressure on the retaining wall. The seepage analysis can be conducted with the flow net method or the finite element method. To simplify the analysis, it is also workable to assume that the seepage is one dimensional.

Problems

4.1 Figure P4.1 shows a two story basement. The soil is silty sand and the groundwater level $H = 3.0$ m. $\gamma = 18$ kN/m^3, $\gamma_{sat} = 22$ kN/m^3, $c' = 0$, $\phi' = 34°$. Compute the total lateral force on the outer wall of the basement (including the resultant and the location of line of action).

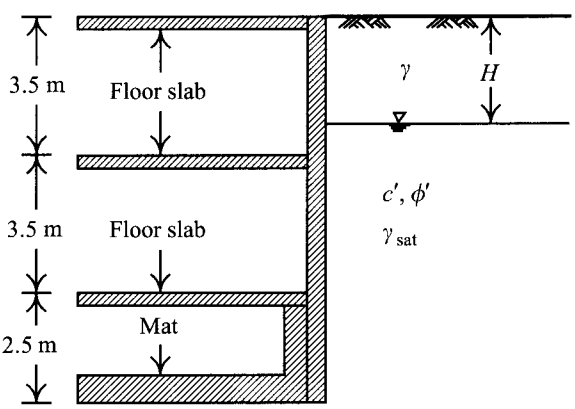

Figure P4.1

4.2 Same as above. Assume that the soil is normally consolidated clay this time. $H = 2.5$ m, $\gamma = 16$ kN/m^3, $\gamma_{sat} = 20$ kN/m^3, $c' = 0$, $\phi' = 32°$, and $s_u = 55$ kN/m^2. Compute the total lateral force on the outer wall of the basement (including the resultant and the location of line of action).

4.3 Assume the soil as shown in Figure P4.3 is sand and the groundwater level is very deep. $H_e = H_p = 13.0$ m, $c' = 0$, $\phi' = 34°$, and $\gamma = 18$ kN/m^3. Compute the active earth pressure using the following earth pressure theories separately (including the resultant and the location of line of action).

a Rankine's earth pressure theory
b Coulomb's earth pressure theory ($\delta = \phi'$)
c Caquot-Kerisel's earth pressure theory ($\delta = \phi'$)

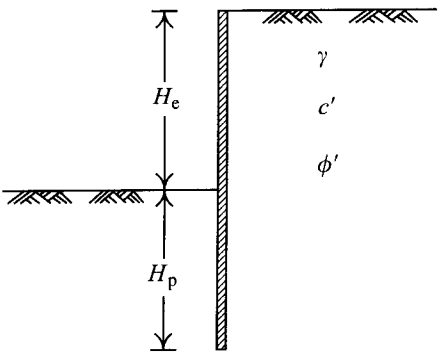

Figure P4.3

4.4 Same as above. If $\delta = \phi'/2$ this time, compute the active earth pressure using Rankine's, Coulomb's, and Caquot-Kerisel's earth pressure theories again.

4.5 Same as Problem 4.3. Compute the passive earth pressure.

4.6 Same as Problem 4.4. Compute the passive earth pressure.

4.7 Assume that the ground as shown in Figure P4.7 consists of clayey soils. $H_1 = 4.0$ m, $s_u = 100$ kN/m^2, $\gamma_{sat1} = 18$ kN/m^3, and $\gamma_{sat2} = 18$ kN/m^3, and $s_u/\sigma'_v = 0.3$. (a) Use Rankine's earth pressure theory (b) use Eq. 4.16 with $c_w = 0.5s_u$ to compute the total active earth pressure (including the resultant and the location of line of action).

4.8 Redo Problem 4.7 assuming $c_w = s_u$ this time.

4.9 Same as Problem 4.7. (a) Use Rankine's earth pressure theory (b) use Eq. 4.18 with $c_w = 0.5s_u$ to compute the total passive earth pressure (including the resultant and the location of line of action).

4.10 Figure P4.10 shows a retaining wall and the soil profile. $H_e = H_p = 9.5$ m, $H_1 = 4.0$ m, $c' = 0$, $\phi' = 32°$, $\gamma = 16$ kN/m^3, $\gamma_{sat} = 18$ kN/m^3, and $s_u/\sigma'_v = 0.35$. The sandy layer has porewater pressure $u = 300$ kN/m^2. Compute the active and passive earth pressures and their locations of line of action using Rankine's earth pressure theory.

4.11 Same as above. Assume that the earth pressure in the sandy layer is computed according to Caquot-Kerisel's theory. The active and passive earth pressures for the clayey layer are computed following Eqs 4.16 and 4.18 ($c_w = 0.5s_u$). Compute the lateral forces on the active and passive sides.

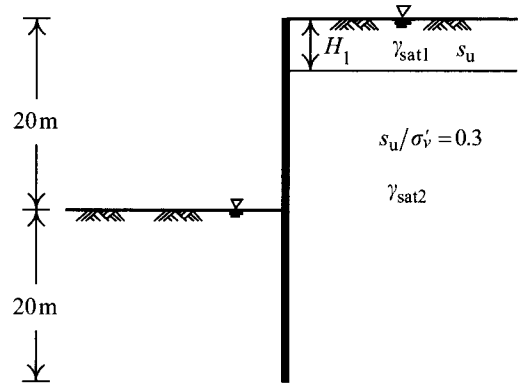

Figure P4.7

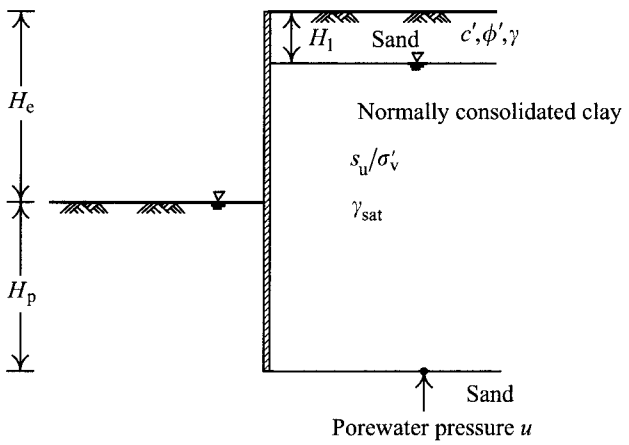

Figure P4.10

4.12 Redo Problem 4.10. Assume that $H_e = H_p = 15$ m, $H_1 = 5.0$ m, $c' = 0$, $\phi' = 35°$, $\gamma = 14$ kN/m^3, $\gamma_{sat} = 20$ kN/m^3, and $s_u/\sigma'_v = 0.30$. The porewater pressure in the sandy layer is $u = 300$ kN/m^2.

4.13 Figure P4.13 shows a clayey layer with a line load of Q_ℓ. The soil above the groundwater level is saturated. $H_e = H_p = 10$ m, $d_j = 1.0$ m, $\gamma_{sat} = 18$ kN/m^3, $s_u = 20$ kN/m^2, $Q_\ell = 500$ kN/m, $d = 3.0$ m. Compute the earth pressure induced by the line load and compare the result with Rankine's active earth pressure.

4.14 Same as the previous problem. Assume that the clayey layer is acted on by a point load $Q_p = 500$ kN. Compute the earth pressure on the section nearest to the point load Q_p. Compare the result with Rankine's active earth pressure, too.

4.15 Redo Problem 4.13. Assume that $H_e = H_p = 15$ m, $d_j = 1.0$ m, $\gamma_{sat} = 20$ kN/m^3, $s_u = 20$ kN/m^2, $Q_\ell = 900$ kN/m, $d = 2.0$ m.

4.16 Figure P4.16 shows a retaining wall and the soil profile. Assume that $H_e = H_p = 10$ m, $d_i = 0.5$ m, $d_j = 1.0$ m, $\gamma = 18$ kN/m^3, $\gamma_{sat} = 22$ kN/m^3, $c' = 0$, $\phi' = 34°$.

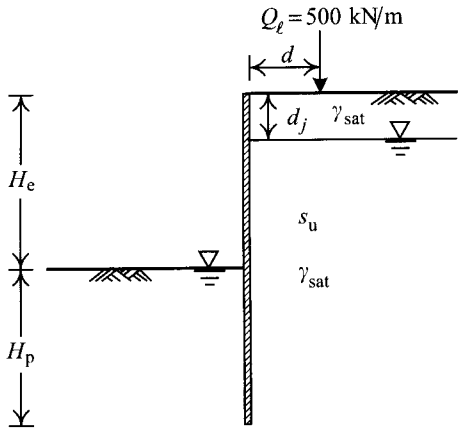

Figure P4.13

According to Caquot-Kerisle's theory, compute the total lateral force, including the resultant and the location of the line of action under the following conditions (assuming $\delta = \phi'$):

a If no seepage occurs.
b If seepage occurs, use the simplified method (assuming that the seepage is one dimensional).
c If seepage occurs, draw the flow net to compute the water pressure.

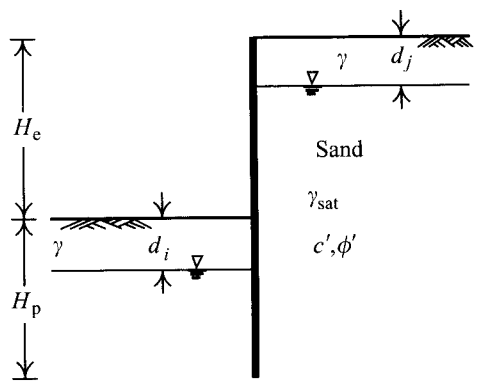

Figure P4.16

4.17 Redo Problem 4.16. Assume $H_e = H_p = 15$ m, $d_i = 0.5$ m, $d_j = 3.0$ m, $\gamma = 12$ kN/m^3, $\gamma_{sat} = 20$ kN/m^3, $c' = 0$, $\phi' = 34°$.

4.18 Redo Problem 4.16. Use Rankine's theory this time.